Search for Squarks and Gluinos in $p\bar{p}$ Collisions at $\sqrt{s} = 1.8$ TeV

S. Abachi,[12] B. Abbott,[33] M. Abolins,[23] B. S. Acharya,[40] I. Adam,[10] D. L. Adams,[34] M. Adams,[15] S. Ahn,[12] H. Aihara,[20] J. Alitti,[36] G. Álvarez,[16] G. A. Alves,[8] E. Amidi,[27] N. Amos,[22] E. W. Anderson,[17] S. H. Aronson,[3] R. Astur,[38] R. E. Avery,[29] A. Baden,[21] V. Balamurali,[30] J. Balderston,[14] B. Baldin,[12] J. Bantly,[4] J. F. Bartlett,[12] K. Bazizi,[7] J. Bendich,[20] S. B. Beri,[31] I. Bertram,[34] V. A. Bezzubov,[32] P. C. Bhat,[12] V. Bhatnagar,[31] M. Bhattacharjee,[11] A. Bischoff,[7] N. Biswas,[30] G. Blazey,[12] S. Blessing,[13] A. Boehnlein,[12] N. I. Bojko,[32] F. Borcherding,[12] J. Borders,[35] C. Boswell,[7] A. Brandt,[12] R. Brock,[23] A. Bross,[12] D. Buchholz,[29] V. S. Burtovoi,[32] J. M. Butler,[12] D. Casey,[35] H. Castilla-Valdez,[9] D. Chakraborty,[38] S.-M. Chang,[27] S. V. Chekulaev,[32] L.-P. Chen,[20] W. Chen,[38] L. Chevalier,[36] S. Chopra,[31] B. C. Choudhary,[7] J. H. Christenson,[12] M. Chung,[15] D. Claes,[38] A. R. Clark,[20] W. G. Cobau,[21] J. Cochran,[7] W. E. Cooper,[12] C. Cretsinger,[35] D. Cullen-Vidal,[4] M. Cummings,[14] D. Cutts,[4] O. I. Dahl,[20] K. De,[41] M. Demarteau,[12] R. Demina,[27] K. Denisenko,[12] N. Denisenko,[12] D. Denisov,[12] S. P. Denisov,[32] W. Dharmaratna,[13] H. T. Diehl,[12] M. Diesburg,[12] G. Di Loreto,[23] R. Dixon,[12] P. Draper,[41] J. Drinkard,[6] Y. Ducros,[36] S. R. Dugad,[40] S. Durston-Johnson,[35] D. Edmunds,[23] A. O. Efimov,[32] J. Ellison,[7] V. D. Elvira,[12,*] R. Engelmann,[38] S. Eno,[21] G. Eppley,[34] P. Ermolov,[24] O. V. Eroshin,[32] V. N. Evdokimov,[32] S. Fahey,[23] T. Fahland,[4] M. Fatyga,[3] M. K. Fatyga,[35] J. Featherly,[3] S. Feher,[38] D. Fein,[2] T. Ferbel,[35] G. Finocchiaro,[38] H. E. Fisk,[12] Yu. Fisyak,[24] E. Flattum,[23] G. E. Forden,[2] M. Fortner,[28] K. C. Frame,[23] P. Franzini,[10] S. Fredriksen,[39] S. Fuess,[12] A. N. Galjaev,[32] E. Gallas,[41] C. S. Gao,[12,†] S. Gao,[12,†] T. L. Geld,[23] R. J. Genik II,[23] K. Genser,[12] C. E. Gerber,[12,‡] B. Gibbard,[3] V. Glebov,[35] S. Glenn,[5] B. Gobbi,[29] M. Goforth,[13] A. Goldschmidt,[20] B. Gomez,[1] P. I. Goncharov,[32] H. Gordon,[3] L. T. Goss,[42] N. Graf,[3] P. D. Grannis,[38] D. R. Green,[12] J. Green,[28] H. Greenlee,[12] G. Griffin,[6] N. Grossman,[12] P. Grudberg,[20] S. Grünendahl,[35] J. A. Guida,[38] J. M. Guida,[3] W. Guryn,[3] S. N. Gurzhiev,[32] Y. E. Gutnikov,[32] N. J. Hadley,[21] H. Haggerty,[12] S. Hagopian,[13] V. Hagopian,[13] K. S. Hahn,[35] R. E. Hall,[6] S. Hansen,[12] R. Hatcher,[23] J. M. Hauptman,[17] D. Hedin,[28] A. P. Heinson,[7] U. Heintz,[12] R. Hernández-Montoya,[9] T. Heuring,[13] R. Hirosky,[13] J. D. Hobbs,[12] B. Hoeneisen,[1,§] J. S. Hoftun,[4] F. Hsieh,[22] Ting Hu,[38] Tong Hu,[16] T. Huehn,[7] S. Igarashi,[12] A. S. Ito,[12] E. James,[2] J. Jaques,[30] S. A. Jerger,[23] J. Z.-Y. Jiang,[38] T. Joffe-Minor,[29] H. Johari,[27] K. Johns,[2] M. Johnson,[12] H. Johnstad,[39] A. Jonckheere,[12] M. Jones,[14] H. Jöstlein,[12] S. Y. Jun,[29] C. K. Jung,[38] S. Kahn,[3] J. S. Kang,[18] R. Kehoe,[30] M. Kelly,[30] A. Kernan,[7] L. Kerth,[20] C. L. Kim,[18] S. K. Kim,[37] A. Klatchko,[13] B. Klima,[12] B. I. Klochkov,[32] C. Klopfenstein,[38] V. I. Klyukhin,[32] V. I. Kochetkov,[32] J. M. Kohli,[31] D. Koltick,[33] A. V. Kostritskiy,[32] J. Kotcher,[3] J. Kourlas,[26] A. V. Kozelov,[32] E. A. Kozlovski,[32] M. R. Krishnaswamy,[40] S. Krzywdzinski,[12] S. Kunori,[21] S. Lami,[38] G. Landsberg,[38] R. E. Lanou,[4] J-F. Lebrat,[36] A. Leflat,[24] H. Li,[38] J. Li,[41] Y. K. Li,[29] Q. Z. Li-Demarteau,[12] J. G. R. Lima,[8] D. Lincoln,[22] S. L. Linn,[13] J. Linnemann,[23] R. Lipton,[12] Y. C. Liu,[29] F. Lobkowicz,[35] S. C. Loken,[20] S. Lökös,[38] L. Lueking,[12] A. L. Lyon,[21] A. K. A. Maciel,[8] R. J. Madaras,[20] R. Madden,[13] I. V. Mandrichenko,[32] Ph. Mangeot,[36] S. Mani,[5] B. Mansoulié,[36] H. S. Mao,[12,†] S. Margulies,[15] R. Markeloff,[28] L. Markosky,[2] T. Marshall,[16] M. I. Martin,[12] M. Marx,[38] B. May,[29] A. A. Mayorov,[32] R. McCarthy,[38] T. McKibben,[15] J. McKinley,[23] H. L. Melanson,[12] J. R. T. de Mello Neto,[8] K. W. Merritt,[12] H. Miettinen,[34] A. Milder,[2] C. Milner,[39] A. Mincer,[26] J. M. de Miranda,[8] C. S. Mishra,[12] M. Mohammadi-Baarmand,[38] N. Mokhov,[12] N. K. Mondal,[40] H. E. Montgomery,[12] P. Mooney,[1] M. Mudan,[26] C. Murphy,[16] C. T. Murphy,[12] F. Nang,[4] M. Narain,[12] V. S. Narasimham,[40] A. Narayanan,[2] H. A. Neal,[22] J. P. Negret,[1] E. Neis,[22] P. Nemethy,[26] D. Nešić,[4] D. Norman,[42] L. Oesch,[22] V. Oguri,[8] E. Oltman,[20] N. Oshima,[12] D. Owen,[23] P. Padley,[34] M. Pang,[17] A. Para,[12] C. H. Park,[12] Y. M. Park,[19] R. Partridge,[4] N. Parua,[40] M. Paterno,[35] J. Perkins,[41] A. Peryshkin,[12] M. Peters,[14] H. Piekarz,[13] Y. Pischalnikov,[33] A. Pluquet,[36] V. M. Podstavkov,[32] B. G. Pope,[23] H. B. Prosper,[13] S. Protopopescu,[3] D. Pušeljić,[20] J. Qian,[22] P. Z. Quintas,[12] R. Raja,[12] S. Rajagopalan,[38] O. Ramirez,[15] M. V. S. Rao,[40] P. A. Rapidis,[12] L. Rasmussen,[38] A. L. Read,[12] S. Reucroft,[27] M. Rijssenbeek,[38] T. Rockwell,[23] N. A. Roe,[20] J. M. R. Roldan,[1] P. Rubinov,[38] R. Ruchti,[30] S. Rusin,[24] J. Rutherfoord,[2] A. Santoro,[8] L. Sawyer,[41] R. D. Schamberger,[38] H. Schellman,[29] D. Schmid,[39] J. Sculli,[26] E. Shabalina,[24] C. Shaffer,[13] H. C. Shankar,[40] R. K. Shivpuri,[11] M. Shupe,[2] J. B. Singh,[31] V. Sirotenko,[28] W. Smart,[12] A. Smith,[2] R. P. Smith,[12] R. Snihur,[29] G. R. Snow,[25] S. Snyder,[38] J. Solomon,[15] P. M. Sood,[31] M. Sosebee,[41] M. Souza,[8] A. L. Spadafora,[20] R. W. Stephens,[41] M. L. Stevenson,[20] D. Stewart,[22] F. Stocker,[39] D. A. Stoianova,[32] D. Stoker,[6] K. Streets,[26] M. Strovink,[20] A. Taketani,[12] P. Tamburello,[21] J. Tarazi,[6] M. Tartaglia,[12] T. L. Taylor,[29] J. Teiger,[36] J. Thompson,[21] T. G. Trippe,[20] P. M. Tuts,[10] N. Varelas,[23] E. W. Varnes,[20] P. R. G. Virador,[20] D. Vititoe,[2] A. A. Volkov,[32] A. P. Vorobiev,[32] H. D. Wahl,[13] J. Wang,[12,†] L. Z. Wang,[12,†] J. Warchol,[30] M. Wayne,[30] H. Weerts,[23] W. A. Wenzel,[20] A. White,[41] J. T. White,[42]

J. A. Wightman,[17] J. Wilcox,[27] S. Willis,[28] S. J. Wimpenny,[7] J. V. D. Wirjawan,[42] Z. Wolf,[39] J. Womersley,[12]
E. Won,[35] D. R. Wood,[12] H. Xu,[4] R. Yamada,[12] P. Yamin,[3] C. Yanagisawa,[38] J. Yang,[26] T. Yasuda,[27] C. Yoshikawa,[14]
S. Youssef,[13] J. Yu,[35] Y. Yu,[37] Y. Zhang,[12,†] Y. H. Zhou,[12,†] Q. Zhu,[26] Y. S. Zhu,[12,†] Z. H. Zhu,[35] D. Zieminska,[16]
A. Zieminski,[16] A. Zinchenko,[17] and A. Zylberstejn[36]

(D0 Collaboration)

[1]*Universidad de los Andes, Bogota, Colombia*
[2]*University of Arizona, Tucson, Arizona 85721*
[3]*Brookhaven National Laboratory, Upton, New York 11973*
[4]*Brown University, Providence, Rhode Island 02912*
[5]*University of California, Davis, California 95616*
[6]*University of California, Irvine, California 92717*
[7]*University of California, Riverside, California 92521*
[8]*LAFEX, Centro Brasileiro de Pesquisas Físicas, Rio de Janeiro, Brazil*
[9]*Centro de Investigacion y de Estudios Avanzados, Mexico City, Mexico*
[10]*Columbia University, New York, New York 10027*
[11]*Delhi University, Delhi, India 110007*
[12]*Fermi National Accelerator Laboratory, Batavia, Illinois 60510*
[13]*Florida State University, Tallahassee, Florida 32306*
[14]*University of Hawaii, Honolulu, Hawaii 96822*
[15]*University of Illinois, Chicago, Illinois 60680*
[16]*Indiana University, Bloomington, Indiana 47405*
[17]*Iowa State University, Ames, Iowa 50011*
[18]*Korea University, Seoul, Korea*
[19]*Kyungsung University, Pusan, Korea*
[20]*Lawrence Berkeley Laboratory, Berkeley, California 94720*
[21]*University of Maryland, College Park, Maryland 20742*
[22]*University of Michigan, Ann Arbor, Michigan 48109*
[23]*Michigan State University, East Lansing, Michigan 48824*
[24]*Moscow State University, Moscow, Russia*
[25]*University of Nebraska, Lincoln, Nebraska 68588*
[26]*New York University, New York, New York 10003*
[27]*Northeastern University, Boston, Massachusetts 02115*
[28]*Northern Illinois University, DeKalb, Illinois 60115*
[29]*Northwestern University, Evanston, Illinois 60208*
[30]*University of Notre Dame, Notre Dame, Indiana 46556*
[31]*University of Panjab, Chandigarh 16-00-14, India*
[32]*Institute for High Energy Physics, 142-284 Protvino, Russia*
[33]*Purdue University, West Lafayette, Indiana 47907*
[34]*Rice University, Houston, Texas 77251*
[35]*University of Rochester, Rochester, New York 14627*
[36]*Commissariat à l'Energie Atomique, DAPNIA/Service de Physique des Particules,*
Centre d'Etudes de Saclay, Saclay, France
[37]*Seoul National University, Seoul, Korea*
[38]*State University of New York, Stony Brook, New York 11794*
[39]*Superconducting Super Collider Laboratory, Dallas, Texas 75237*
[40]*Tata Institute of Fundamental Research, Colaba, Bombay 400005, India*
[41]*University of Texas, Arlington, Texas 76019*
[42]*Texas A&M University, College Station, Texas 77843*

We present a search for events consistent with the production and decay of the squarks and gluinos of the minimal supersymmetric standard model (MSSM) in the D0 detector at the Fermilab Tevatron $p\overline{p}$ collider. We examined data for events containing large missing transverse energy and three or more jets. We observed no excess of events above the expected yield from standard model processes. For a choice of MSSM parameter values, we set a lower limit at the 95% confidence level on the mass of the gluino of 144 GeV/c^2 for all squark masses and a lower limit of 212 GeV/c^2 for equal squark and gluino masses.

PACS numbers: 14.80.Ly, 13.85.Rm

Despite the experimental success of the standard model (SM) there is great interest in looking for evidence of its possible extensions. One attractive extension is supersymmetry (SUSY), a spacetime symmetry which relates

bosons to fermions and introduces a supersymmetric partner (sparticle) for each SM particle. SUSY provides a natural solution to the fine-tuning problem of the SM and yields a candidate for dark matter. It also allows supersymmetrized grand unified theories (SUSY-GUT's) that are consistent with experimental measurements of the proton lifetime limits and can unify the U(1), SU(2), and SU(3) couplings of the SM at the GUT scale. The supersymmetrized SM with arbitrary SUSY-breaking terms [1], however, leads to a plethora of new parameters which make phenomenological analysis of the experimental data intractable. Such analyses become more feasible if one assumes that the many SUSY-breaking terms are related as in a supergravity (SUGRA) GUT model.

In this Letter we present a search, in the framework of the SUGRA-inspired MSSM, for squarks $\tilde{q}$ and gluinos $\tilde{g}$, which are the SUSY partners of the quarks and gluons of the SM. We assume conservation of R parity, a symmetry which has multiplicative quantum numbers $+1$ for SM particles and -1 for sparticles, and, therefore, the sparticles must be produced in pairs in $p\overline{p}$ collisions and the lightest supersymmetric particle (LSP) is stable [2].

The data used in this analysis were obtained with the D0 detector at the Fermilab Tevatron collider operating at a $p\overline{p}$ center-of-mass energy of 1.8 TeV. The total integrated luminosity collected by D0 during the Tevatron 1992–1993 run was 13.5 ± 1.6 pb^{-1}. The D0 detector has three major subsystems: central tracking detectors, a nearly hermetic liquid argon calorimeter, and a muon spectrometer. A detailed description of the D0 detector and data collection systems can be found elsewhere [3].

The expected cross section for $\tilde{q}$ and $\tilde{g}$ production at the Tevatron is large. For example, for $m_{\tilde{q}} = m_{\tilde{g}} = 200$ GeV/c^2 the expected combined cross section for gluino and squark production is approximately 10 pb. There are three major production mechanisms for squarks and gluinos: gluino pair production, squark pair production, and associated gluino and squark production. The details of the decay modes for squarks and gluinos depend on the input parameters of the model. In general, the decay of each squark or gluino involves intermediate state charginos and neutralinos and results in a final state consisting of a LSP and jets, with or without leptons. Since the LSP is stable and does not interact in the detector, the production of a high E_T LSP results in large missing transverse energy ($\not{E}_T$).

In this analysis, we use the excellent jet energy resolution and coverage of the D0 calorimeter to look for events with three or more jets and large $\not{E}_T$ in the absence of leptons. The major backgrounds to this event signature are the leptonic decays of W and Z bosons produced in association with multiple jets, where the leptons are misidentified or not detected. Poorly measured multijet events can also contribute to the background, but their contribution falls very rapidly with increasing $\not{E}_T$. Jets are found from calorimeter information using a cone algorithm of radius 0.5 in η-ϕ space [4]. $\not{E}_T$ is calculated from the

energy deposits in the individual calorimeter cells and is defined to be the negative of the vector sum of the cell transverse energies.

We trigger on events with combinations of $\not{E}_T$ and jet candidates; we use $\not{E}_T$ thresholds ranging from 20 to 40 GeV. In the off-line selection, we initially filter the data by requiring $\not{E}_T \gtrsim 25$ GeV and by applying other cuts similar to the event selection cuts described below. A more detailed description of the trigger, event filtering, and reconstruction algorithms for electrons, muons, jets, and $\not{E}_T$ is given in Ref. [5].

Events with multiple interactions can introduce large uncertainties in jets E_T and $\not{E}_T$ since the angles assigned to calorimeter energy clusters can be incorrect. We require that only one reconstructed vertex be found, and thus we reduce the effective luminosity to 7.1 ± 0.9 pb^{-1}. The uncertainty includes the uncertainty in the single vertex detection efficiency, the misidentification probability of a multiple interaction as a single interaction, and the uncertainty in the luminosity (12% systematic), all added in quadrature. After trigger selection and an initial filtering of the data sample, this requirement yields 3811 events.

In order to assure that the event is well contained in the calorimeter, we require the z location of the event vertex to be within ± 70 cm of the nominal beam collision position (the z axis is parallel to the proton beam). A total of 3730 events pass this cut.

The most powerful parameter for distinguishing the $\tilde{q}/\tilde{g}$ events from the known SM backgrounds is $\not{E}_T$. We require $\not{E}_T > 75$ GeV to reduce the backgrounds significantly, especially the multijet background, while keeping substantial signal efficiency. Our on-line trigger is fully efficient for events that pass this cut. This cut results in 107 remaining events.

We next require that there be three or more jets with $E_T > 25$ GeV and $|\eta| \leq 3.5$. We reject any event that contains a jet with $E_T > 15$ GeV in the same η range which fails any of the following quality criteria: (1) $0.10 <$ electromagnetic fraction of the jet $E_T < 0.90$, (2) the ratio of the highest cell energy to the next highest < 10, and (3) the fraction of E_T deposited in the outermost calorimeter layer (which has a depth of 3.2 interaction lengths) < 0.4. These requirements are designed to distinguish real jets from jets formed around noisy calorimeter cells and jets induced by particles from the main ring accelerator bypass through the outer layers of the D0 calorimeter. Although the D0 calorimeter is nearly hermetic, in the region $1.1 < |\eta| < 1.4$ there is no fine segmentation suitable for electromagnetic calorimetry, and the energy resolution is compromised. We reject events in which the leading E_T jet appears in this region. Large $\not{E}_T$ events with mismeasured nonleading jets in this region do not contribute significantly to the background. A total of 32 events pass these cuts.

Some events with little true $\not{E}_T$ are found to have large measured $\not{E}_T$ due to fluctuations in the measured jet energies. To remove such events, we order the jets in

terms of decreasing E_T and define $\delta\phi_k$ as the azimuthal angle between jet k and the $\not{E}_T$ vector. We reject events that have $\not{E}_T$ opposite or adjacent ($\delta\phi_k > \pi - 0.1$ or $\delta\phi_k < 0.1$ for $k = 1, 2, 3$) to any of the three leading jets. Furthermore, we reject those events in which a fluctuation of the second jet masks the correlation with the first jet ($\sqrt{(\delta\phi_1 - \pi)^2 + (\delta\phi_2)^2} < 0.5$). These cuts are effective in rejecting the multijet background. There remain 22 events after these cuts.

The decays $W \to \ell\overline{\nu}$ and $Z \to \tau^+\tau^-$ (with one of the taus decaying leptonically) are significant SM sources of real $\not{E}_T$. To remove these events we require that there be no electrons with $E_T > 20$ GeV and no muons with $p_T > 15$ GeV/c. A total of 17 events survive this cut.

Finally, these 17 candidate events are studied for anomalies, and we find three events which cannot be produced by the signal or the backgrounds we are considering. The first of these contains a muon, consistent with a high energy cosmic ray, which escapes our muon rejection cuts because it is significantly out of time. It interacts in the calorimeter to produce a large visible energy and large apparent $\not{E}_T$. In the other two anomalous events, the vertex algorithm fails to construct a vertex near the true origin of the jets in the event. Instead it mistakenly constructs a vertex far from the origin. When the events are reconstructed using the origin to calculate $\not{E}_T$, the fail the 75 GeV $\not{E}_T$ cut. We reject these three events, which leaves us with a final candidate sample of 14 events. Figure 1 shows the $\not{E}_T$ distribution of these events.

To estimate the W/Z associated background contributions to the final candidate sample, we use a Monte Carlo (MC) package composed of the VECBOS [6] generator for parton generation and a modified version of ISAJET [7] for subsequent fragmentation and hadronization. We produce events with either a W or a Z and one, two, or three jets. These events are then passed through a simulation of the D0 detector based on the GEANT [8] program. We also
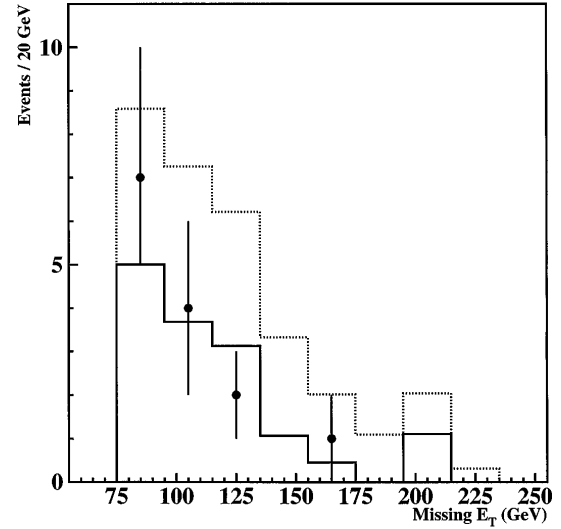

FIG. 1. The $\not{E}_T$ distribution of the final 14 candidate events (solid circles with error bars), the background simulations (solid line, normalized to the same luminosity as the data), and a signal sample with $m_{\tilde{g}} = m_{\tilde{q}} = 200$ GeV/c^2 combined with the background (dashed line, normalized to the same luminosity as the data).

use data to determine background efficiencies for the jet quality and muon identification cuts in order to minimize possible discrepancies between data and MC events. Our W/Z background estimates are shown in Table I. The cross sections are determined with VECBOS. The statistical uncertainties reflect the small statistical uncertainties in the VECBOS cross section and the uncertainties in the branching fractions from the Particle Data Group [9]; the systematic uncertainties include the 10% per jet systematic uncertainty in the cross section from VECBOS. The dominant source of the systematic uncertainty in the detection efficiencies is the jet energy scale uncertainty ($\pm 5\%$) [10]. The systematic uncertainties in the expected number of events include the uncertainty in the luminosity. The sum of our estimates for all W and Z backgrounds

TABLE I. Predicted backgrounds from W and Z production in association with jets. $\sigma_{VB}B$ is the product of the VECBOS cross section and the branching fraction for the process, ε_B is the efficiency, and N_{pred} is the predicted number of events in 7.1 pb^{-1}. The notation τ_ℓ indicates the leptonic decay of the τ; the notation τ_h indicates the hadronic decay of the τ. For each channel the number of associated jets is 3 minus the number of hadronic decays of the τ in that channel.

Channel	$\sigma_{VB}B$ (pb)	ε_B (%)	N_{pred}
$W \to e\overline{\nu}$	$54.2 \pm 4.7 \pm 16.2$	$0.59 \pm 0.14^{+0.03}_{-0.06}$	$2.28 \pm 0.55^{+0.69}_{-0.72}$
$W \to \mu\overline{\nu}$	$54.2 \pm 9.6 \pm 16.3$	$1.31 \pm 0.23^{+0.52}_{-0.28}$	$5.08 \pm 1.24^{+2.45}_{-1.84}$
$W \to \tau_h\overline{\nu}$	$116.5 \pm 17.7 \pm 23.3$	$0.26 \pm 0.07^{+0.15}_{-0.04}$	$2.16 \pm 0.66^{+1.23}_{-0.52}$
$W \to \tau_\ell\overline{\nu}$	$19.4 \pm 3.0 \pm 5.8$	$1.33 \pm 0.27^{+0.34}_{-0.37}$	$1.84 \pm 0.46^{+0.71}_{-0.73}$
$Z \to e\overline{e}$	$4.96 \pm 0.05 \pm 1.5$	~ 0	~ 0
$Z \to \mu\overline{\mu}$	$4.95 \pm 0.07 \pm 1.5$	$1.34 \pm 0.31^{+0.26}_{-0.17}$	$0.47 \pm 0.11^{+0.17}_{-0.15}$
$Z \to \nu\overline{\nu}$	$30.0 \pm 0.6 \pm 9.0$	$2.15 \pm 0.33^{+0.49}_{-1.0}$	$4.59 \pm 0.68^{+1.70}_{-2.49}$
$Z \to \tau_h\overline{\tau}_h$	$22.5 \pm 0.3 \pm 2.3$	~ 0	~ 0
$Z \to \tau_h\overline{\tau}_\ell$	$7.6 \pm 0.19 \pm 1.5$	$0.46 \pm 0.10^{+0.11}_{-0.13}$	$0.25 \pm 0.05^{+0.08}_{-0.08}$
$Z \to \tau_\ell\overline{\tau}_\ell$	$0.62 \pm 0.03 \pm 0.19$	$0.95 \pm 0.26^{+0.21}_{-0.18}$	$0.04 \pm 0.01^{+0.02}_{-0.02}$
Total			$16.7 \pm 1.7^{+7.0}_{-6.6}$

is $16.7 \pm 1.7^{+7.0}_{-6.6}$ events. We combine the statistical uncertainties of each channel in quadrature but add the systematic uncertainties linearly.

To estimate the multijet background contributions to the final candidate sample, we use a multijet data sample collected with a trigger requiring one 0.7 cone jet with $E_T > 20$ GeV. First, we fit the $\not{E}_T$ spectrum of the sample after applying the same data selection cuts except the $\not{E}_T$ cut and the three or more jet requirement in order to keep a sufficient number of events for the fit. Then, we determine the fraction of the events passing the three or more jet requirement as a function of $\not{E}_T$ of the sample. The fitted result yields a total of 0.42 ± 0.37 expected multijet background events in the candidate sample.

The combined total number of expected W/Z associated and multijet background events is $17.1 \pm 1.8^{+7.0}_{-6.6}$, which is consistent with the observed number (14) of candidate events. Thus, we observe no excess of events above the SM predictions.

In order to interpret the null search results for $\tilde{q}/\tilde{g}$ events as an excluded region in the $m_{\tilde{g}}$-$m_{\tilde{q}}$ plane, $\tilde{q}/\tilde{g}$ events are generated at various masses with the ISASUSY generator [11] combined with the detector simulation programs described above. ISASUSY is an extension of the generator ISAJET and models the production of SUSY particles in $p\overline{p}$ collisions and their subsequent decays in the framework of the SUGRA-inspired MSSM. The version of ISASUSY we use models only squark and gluino production. Top squark $\tilde{t}$ production is not included, and the other five flavors of left- and right-handed squarks are assumed to be mass degenerate. Therefore, our search places a limit on the masses of the heavy squarks, not on the possibly lighter $\tilde{t}$. In this analysis, we use the following low energy input parameters. We set the charged Higgs mass $m_{H^+} = 500$ GeV/c^2, the ratio of the vacuum expectation values of the two Higgs doublets $\tan\beta = 2$, the Higgsino mass mixing parameter $\mu = -250$ GeV/c^2, and the top quark mass $m_t = 140$ GeV/c^2. We vary both the squark mass $m_{\tilde{q}}$ and the gluino mass $m_{\tilde{g}}$. We set the common slepton $\tilde{\ell}$ mass to be the same as the common squark mass.

The signal detection efficiencies ϵ are determined for a grid of values in the $m_{\tilde{g}}$-$m_{\tilde{q}}$ plane. Example efficiencies are $(19 \pm 2)\%$, $(6 \pm 2)\%$, and $(8 \pm 2)\%$ for $(m_{\tilde{g}}, m_{\tilde{q}}) = (200$ GeV/$c^2, 200$ GeV/$c^2)$, $(150,400)$, and $(400,150)$, respectively. We interpolate to find efficiencies between grid points. The trigger is fully efficient for events that pass our off-line cuts.

To determine our cross-section limit, we compute the observed signal cross section σ: $\sigma = (N - n_b)/(L\epsilon)$, where N is the number of candidate events observed in the data, n_b is the predicted number of background events, and L is the integrated luminosity. We then obtain a conservative 95% C.L. upper limit using our estimated uncertainties on all quantities [5]. The cross-section limits are 8.9, 29, and 22 pb for $(m_{\tilde{g}}, m_{\tilde{q}}) = (200$ GeV/$c^2, 200$ GeV/$c^2)$, $(150,400)$, and $(400,150)$, respectively.

To present our cross-section limit as a gluino and squark mass limit, we used the calculation of the production cross section obtained with ISASUSY which employs the EHLQ2 parton distribution function [12] with a renormalization and factorization scale of $\hat{s}$. The cross section varies by $\pm 30\%$ when the scale is varied from $4\hat{s}$ to $\hat{s}/4$ but varies little with the choice of parton distribution function. Figure 2 shows the region in the $m_{\tilde{g}}$-$m_{\tilde{q}}$ plane excluded by our search at the 95% C.L. [13], along with the previous results of other experiments [14]. In the limit of $m_{\tilde{q}} \gg m_{\tilde{g}}$, gluino pair production dominates the other two processes, and the gluino decay patterns are insensitive to further increase in the squark mass. In this region we produce an asymptotic limit of $m_{\tilde{g}} > 144$ GeV/c^2. In the case of equal squark and gluino masses, we produce a limit $m_{\tilde{g}} = m_{\tilde{q}} > 212$ GeV/c^2. The highest gluino mass excluded is 547 GeV/c^2 for a 120 GeV/c^2 squark mass. Variation of $\tan\beta$ and μ over the range preferred in SUGRA-GUT models is expected to lead to variations in mass bounds of approximately 10% [15]. Our results are insensitive to reasonable variations in the choice of m_{H^+} and m_t and apply not only for $m_{\tilde{\ell}} = m_{\tilde{q}}$ but also for $m_{\tilde{\ell}} > m_{\tilde{q}}$.

In conclusion, we observe 14 events with $\not{E}_T > 75$ GeV, with three or more jets, and with no identified electrons or muons. The observed number of candidate events is consistent with the SM predictions. We interpret the null search result for squark and gluino events in the framework of SUGRA-inspired MSSM as an excluded
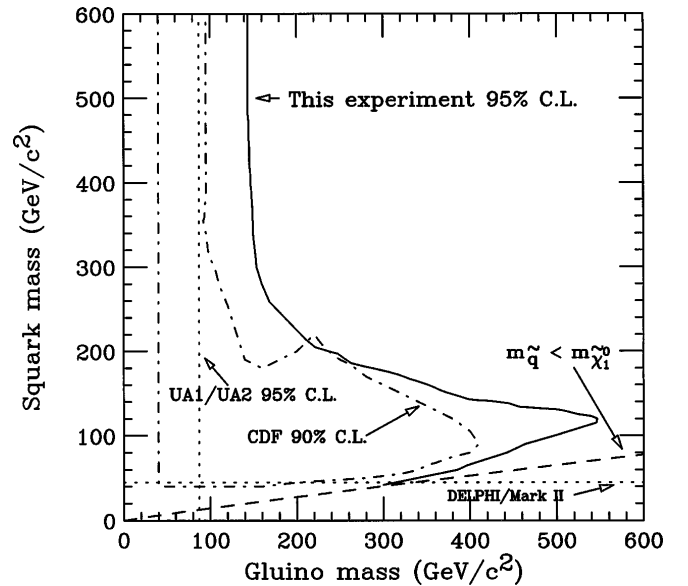

FIG. 2. Current squark and gluino mass limits. Left of the solid line is the D0 95% C.L. excluded region. Inside the dash-dotted line is the CDF 90% C.L. excluded region. Left of the vertical dotted line is the gluino mass region excluded by UA1 and UA2. Below the horizontal dotted line is the squark mass region excluded by the DELPHI and Mark II experiments. Below the dashed line is the model excluded region where the squark mass is less than that of the lightest neutralino.

region in the $m_{\tilde{g}}$-$m_{\tilde{q}}$ plane. We significantly extend the high mass region excluded by other experiments.

*Visitor from CONICET, Argentina.

†Visitor from IHEP, Beijing, China.

‡Visitor from Universidad de Buenos Aires, Argentina.

§Visitor from Univ. San Francisco de Quito, Ecuador.

[1] X. Tata, in *The Standard Model and Beyond,* edited by J. Kim (World Scientific, Singapore, 1991); H. Nilles, Phys. Rep. **110**, 1 (1984); P. Nath *et al., Applied N = 1 Supergravity,* ICTP Series in Theoretical Physics Vol. 1 (World Scientific, Singapore, 1984); H. Haber and G. Kane, Phys. Rep. **117**, 75 (1985).

[2] In these models the lightest neutralino $\tilde{\chi}_1^0$ is the LSP.

[3] D0 Collaboration, S. Abachi *et al.,* Nucl. Instrum. Methods Phys. Res., Sect. A **338**, 185 (1994), and references therein.

[4] Pseudorapidity $\eta = \tanh^{-1}(\cos\theta)$; θ, ϕ = polar, azimuthal angle.

[5] M. Paterno, Ph.D. dissertation, The State University of New York at Stony Brook, 1994 (unpublished, on World Wide Web via http://fnnews.fnal.gov/).

[6] F. Berends *et al.,* Nucl. Phys. **B357**, 32 (1991).

[7] F. Paige and S. D. Protopopescu, Brookhaven National Laboratory Report No. 38304, 1986 (unpublished). We use ISAJET V6.49.

[8] R. Brun and F. Carminati, CERN Program Library Long Writeup W5013, 1993 (unpublished).

[9] Particle Data Group, Phys. Rev. D **50**, S1 (1994).

[10] D0 Collaboration, S. Abachi *et al.,* Report No. FERMILAB-PUB-1995/020-E.

[11] H. Baer *et al.,* in *Proceedings of the Workshop on Physics at Current Accelerators and Supercolliders,* edited by J. Hewett *et al.* (Argonne National Laboratory, Argonne, IL, 1993), p. 703.

[12] E. Eichten *et al.,* Rev. Mod. Phys. **58**, 1965 (1986).

[13] At the 90% C.L., the excluded region extends approximately 5 GeV/c^2 further.

[14] CDF Collaboration, F. Abe *et al.,* Phys. Rev. Lett. **69**, 3439 (1992); DELPHI Collaboration, P. Abreu *et al.,* Phys. Lett. B **247**, 148 (1990); Mark II Collaboration, T. Barklow *et al.,* Phys. Rev. Lett. **64**, 2984 (1990); UA1 Collaboration, C. Albajar *et al.,* Phys. Lett. B **198**, 261 (1987); UA2 Collaboration, J. Alitti *et al.,* Phys. Lett. B **235**, 363 (1990).

[15] H. Baer *et al.,* Phys. Rev. Lett. **63**, 352 (1989); Phys. Rev. D **41**, 906 (1990); **44**, 207 (1991).